Collection de notes internes de la Direction des Etudes et Recherches

ETUDE DES MECANISMES DE LA CORROSION SOUS CONTRAINTE DE L'ALLIAGE 600 DANS L'EAU A HAUTE TEMPERATURE

STRESS CORROSION CRACKING OF ALLOY 600 IN HIGH TEMPERATURE WATER : A STUDY OF MECHANISMS

EDF
Electricité de France

EDF
Electricité de France

Direction des Etudes et Recherches

SERVICE RÉACTEURS NUCLÉAIRES ET ECHANGEURS
Département Etude des Matériaux

Décembre 1992

BOURSIER J.M.
DE BOUVIER O.
GRAS J.M.
NOEL D.
VAILLANT F.

ETUDE DES MECANISMES DE LA CORROSION SOUS CONTRAINTE DE L'ALLIAGE 600 DANS L'EAU A HAUTE TEMPERATURE

STRESS CORROSION CRACKING OF ALLOY 600 IN HIGH TEMPERATURE WATER : A STUDY OF MECHANISMS

Pages : 18

93NB00051

Diffusion : J.-M. Lecœuvre
EDF-DER
Service IPN. Département SID
1, avenue du Général-de-Gaulle
92141 Clamart Cedex

ISSN 1161-0611

SYNTHÈSE :

Une étude de la résistance à la corrosion sous contrainte de l'Alliage 600 dans l'eau à haute température a été entreprise afin de mieux connaître les différents stades de la fissuration et l'influence de divers paramètres. La compatibilité des résultats avec les principaux mécanismes de corrosion sous contrainte a été examinée.

Les résultats mettent en évidence trois stades dans la fissuration : une période d'amorçage, puis une période de propagation lente suivie d'une période de propagation rapide. Des essais séparant l'effet de la contrainte et de la vitesse de déformation montrent que la vitesse de déformation est le principal paramètre contrôlant la propagation de la fissuration.

Une surpression d'hydrogène augmente la vitesse de propagation jusqu'à 1 ou 4 bar, mais provoque une forte diminution entre 4 et 20 bar. L'absorption de l'hydrogène dans le métal ne se corrèle ni avec la surpression d'hydrogène dans l'eau, ni avec la sévérité de l'essai : un mécanisme de type fragilisation par l'hydrogène est donc peu probable. Aucun effet défavorable de l'oxygène (suppression de 4 bar) n'a été observé, que ce soit sur un état non traité thermiquement ou sur un état sensibilisé.

Aucun des mécanismes classiques de la corrosion sous contrainte, qu'il s'agisse de la fissuration induite par l'hydrogène ou de la dissolution-passivation, ne peut décrire de façon correcte les résultats. Les examens fractographiques et l'influence du milieu sur le fluage de l'Alliage 600 suggèrent que d'autres mécanismes plus récents, impliquant une interaction entre la dissolution et la plasticité, doivent être pris en considération.

1993

93NB00051

EXECUTIVE SUMMARY :

Investigations of the stress corrosion cracking behaviour of Alloy 600 tubing in high temperature water were performed in order to get a precise knowledge of the different stages of the cracking and their dependance on various parameters. The compatibility of the results with the main mechanisms to be considered was examined.

Results showed three stages in the cracking : a true incubation time, a slow-rate propagation period followed by a rapid-propagation stage. Tests separating stress and strain rate contributions show that the strain rate is the main parameter which controls the crack propagation.

The hydrogen overpressure was found to increase the crack growth rate up to 1-4 bar, but a strong decrease is observed from 4 to 20 bar. Analysis of the hydrogen ingress in the metal showed that it is neither correlated to the hydrogen overpressure nor to the severity of cracking ; so cracking resulting from an hydrogen-model is unlikely. No detrimental effect of oxygen (4 bar) was noticed both in the mill-annealed and the sensitized conditions.

Finally, none of the classical mechanisms, neither hydrogen-assisted cracking nor slip-step dissolution, can correctly describe the observed behaviour. Some fractographic examinations, and an influence of primary water on the creep rate of Alloy 600, lead to consider that other recent mechanisms, involving an interaction between dissolution and plasticity, have to be considered.

93NB00051

SCC OF ALLOY 600 IN HIGH TEMPERATURE WATER : A STUDY OF MECHANISMS

J.M. Boursier, O. de Bouvier, J.M. Gras, D. Noel, R. Rios* and F. Vaillant
Électricité de France, Département Étude des Matériaux, Les Renardières
77250 - Moret-sur-Loing, France

1 - INTRODUCTION

The cracking of Alloy 600 steam generators tubing is a great concern for pressurized water reactors (PWR). Intergranular stress corrosion cracking (IGSCC) occurs in heavily cold-worked areas, mainly in roll-transition areas where the residual stresses from manufacture are the greatest. As early as 1959 Coriou et al proved that solution-annealed nickel base alloys are susceptible to IGSCC in de-aerated water at high temperatures [1]. During the past two decades, numerous papers have been published concerning Alloy 600 IGSCC in PWR [2-5], and quantitative IGSCC modelling has been produced [6-7], but the mechanism that controls IGSCC in nickel base alloys has yet to be clearly identified.

SCC of steam generator tubing materials is generally explained either by film/rupture dissolution model or by hydrogen-induced cracking mechanisms. Film-induced-cleavage or mechanisms of brittle rupture induced by interaction between corrosion and plasticity (local softening) were more recently proposed, but their relevance for Alloy 600 IGSCC is a subject of debate. Supporting evidence and attributes for slip dissolution model and hydrogen-induced cracking are outlined here, focusing on IGSCC in pure/primary water.

As other authors have already pointed out, it will first be noted that both mechanisms are not necessarily incompatible. They may even act simultaneously, in various proportions depending on environment (potential, pH), material etc... The slip-step dissolution and the hydrogen embrittlement models of SCC depend on similar rate-controlling parameters, and it is difficult to discriminate experimentally between these two mechanisms [8]. On the other hand, since corrosion involves successive stages (initiation without cracking, slow-cracking propagation and fast-cracking propagation) [5], it is not necessary, *a priori*, to assume that cracking is controlled by the same mechanism during the different stages, as passing from one stage to another may be the result of a change in the dominant mechanism.

---

* also Université de Lille I, Laboratoire de Métallurgie Physique, Bât. C6, 59655-Villeneuve d'Ascq, France

Slip-step dissolution models implying passivation, oxide rupture events controlled by the strain rate and oxidation/dissolution following oxide rupture have been widely considered, as in other cases of SCC. The validity of such a mechanism concerning the IGSCC of Alloy 600 in pure/primary water was discussed by numerous authors, but their opinions are less conclusive than about IGSCC of sensitized 304 stainless steels in oxygenated high temperature BWR water. Some arguments are in favour of a dissolution mechanism [8-11] : (i) cracking requires the presence of a passive film, (ii) the crack growth rate as measured by CERTs according to the law $V = A(n) (\dot{\varepsilon}_{CT})^n$ is consistent with the elemental dissolution transient on the damaged film $i = i_0 (t/t_0)^{-n}$ [8-9] : (iii) the rate of dissolution can be influenced by several factors such as potential, ions in solution, material composition (especially chromium content) and the metal's grain boundary state. So in the presence of intergranular carbides, passivation occurs more easily and the passive film is more protective than in the absence of intergranular carbides ; carbon in solid solution gives rise to a more difficult passivation and enhances dissolution of Alloy 600 [12].
Slip-step oxidation mechanism controled by mass transfer and solubility of iron could also be considered to account for the influence of pH and hydrogen on cracking [13].

However, other observations are questionable : (i) cracking is inhibited by anodic polarization and increased by cathodic potentials, (ii) alloy sensitization is not detrimental in pure or primary water.

The hydrogen induced cracking mechanisms are supported by the detrimental effect of molecular hydrogen dissolved in water or mixed with steam on the IGSCC resistance of Alloy 600. There is an intricate dependence of IGSCC on the hydrogen partial pressure and the potential : IGSCC only occurs at potentials below approximately - 835 mV_{SHE}, independently on the hydrogen partial pressure [14]. This threshold potential is close to the equilibrium potential of hydrogen, showing that hydrogen seems to play a decisive role in the cracking of Alloy 600 in high-temperature water. Furthermore, high concentration of hydrogen was found in the stressed parts of cracked tensile specimens.

However, in dry hydrogen gas, no failure of mill-annealed Alloy 600 has been found to occur at 400°C at a pressure of 6.3 MPa ; additionnally, in wet hydrogen gas, mill-annealed and heat-treated Alloy 600 show a behavior opposite to that observed in systems with high temperature water and steam : rupture of heat-treated material is brittle intergranular whereas rupture of mill-annealed material is ductile transgranular [5]. It is not yet fully possible to definitively make a conclusion on the true effect of hydrogen on Alloy 600 cracking in pure/primary water. Indeed, hydrogen may involve two effects : (i) modification of environment (shift of corrosion potential to less noble values, modification of the process of metal dissolution, modification of the protective properties of the oxide layer), (ii) intrinsic embrittlement effect. Moreover the combination of hydrogen concentration and triaxial stress state does not imply that it is the only cause of cracking. A different explanation of the intrinsic damaging effect of hydrogen on Alloy 600 in deaerated water or steam at high temperature has been suggested recently [15] : cracks are initiated by the nucleation of a high density of bubbles on the grain boundary under the combined action of the applied stress and high pressure of methane formed from carbon in solution reacting with hydrogen injected by corrosion. This mechanism (void-linkage model) involves no grain boundary dissolution of the metal, the only role of corrosion being injection of hydrogen atoms at a high fugacity.

Theories of brittle rupture induced by interaction between corrosion and plasticity (local softening) were more recently proposed [16-19]. They first concerned transgranular cracking of stainless steels. A recent work examined their relevance for intergranular cracking of nickel alloys [20], and concluded that these models could possibly be applied in that case.

The aim of this paper is to review some critical aspects of Alloy 600 IGSCC in pure/primary water in order to better understand the phenomenon, with particular emphasis on the role of strain rate and of hydrogen, and to discuss the mechanisms which could account for the obtained experimental results.

2- EXPERIMENTAL

Materials

Three heats of Alloy 600 tubing (ϕ 22.2 x 1.27 mm) were used for the study. Their main characteristics are presented in table I, and their susceptibility to SCC is indicated in table II. The precipitates of the tube 6E (not susceptible to SCC) are mostly intergranular ; the precipitates of the tube 6L (susceptible to SCC) and those of the tube 6.242.R (very susceptible) are mostly intragranular. The tube 6.242.R was also tested after a thermal treatment lasting one hour at 700°C. This treatment was performed in order to sensitize the tube to intergranular corrosion. After this treatment, a corrosion test as defined by the ASTM G 28 standard gave rise to a throughwall intergranular corrosion.

Table I : Main characteristics of studied Alloy 600 tubings

Name of tubes	Carbon content (%)	MA temperature (°C)	ASTM grain size	Yield stress at 350°C (MPa)
6E	0.033	1,070	8 (22 μm)	280
6L	0.026	980	10 (11 μm)	330
6.242.R	0.030	915	10 (11 μm)	290

Table II : Alloy 600 tubes sensitivity in relation with their metallurgical structure (360°C, primary water + 4 bar hydrogen overpressure at 125°C)

	RUB tests	Constant load tests		CERT *
Name of tubes	Time to cracking (h)	Nominal stress (MPa)	Time to cracking (h)	Crack depth (μm)
6E	>36,000	-	-	10
6L	<1,000	684	822	100
6.242.R	<500	570	900	325

* Constant extension rate : 5×10^{-8} s^{-1}, 50 μm electropolished tube

Stress corrosion tests

Stress corrosion tests were Reverse U-Bend tests (RUB), Constant Extension Rate tests (CERTs) and constant-load tests. The strain rate for CERTs was between 5×10^{-9} and 10^{-6} s^{-1}. The applied stress in constant-load tests was from 450 to 680 MPa.

The environment was primary water (1,000 ppm B as boric acid, 2 ppm Li as lithium hydroxide) at 360°C. The tests were carried out with 0 to 20 bar-hydrogen overpressure in most cases, or in some cases with a 4 bar-oxygen overpressure. The gas was introduced at 125°C, and the overpressure at test temperature was calculated, taking into account water and gas dilatation phenomenons, and the solubility coefficient of hydrogen at 360°C. The solubility data were taken from reference [21].

Tensile specimens were cut longitudinally in the tubes. The section of specimens was 3.5 x 1.27 mm^2 with a gauge length of 88 mm. The ID and OD surfaces of the tubing were either in the as-received or electropolished condition. In the as-received condition, the OD surface shows strain-hardened superficial layer of 70 to 90 μm-depth, and a residual compressive stress level from 300 to 400 MPa ; the ID surface shows strain-hardened superficial layer of 15 to 20 μm-depth, and a residual compressive stress level from 100 to 200 MPa (measurements by X-ray diffraction). The electropolishing suppressed these superficial layers.

Creep tests

Creep tests were carried out in air at 350 or 360°C. Specimens were cut longitudinally in the tubes, with a gauge length of 34 mm. They were held for approximativaly 20 hours at the test temperature before a stress between 450 and 650 MPa was applied.

Experimental measurement

Except for the RUB tests, strain elongation and stress were measured during the tests. Fracture surfaces were examined by SEM. Moreover, the entire specimens were examined on micrographical sections in order to evaluate the number and the depth of cracks. This crack distribution was automatically determined by image analysis, in order to estimate propagation rates for the different stages of cracking. For this estimation, the mathematical method developped by Santarini [22] was used. Image analysis gave a good correlation between calculated and real crack depth for cracks longer than 10 μm, and calculated propagation rates were in a fairly good agreement with those measured by interrupted tests during the slow (V_1) and the rapid (V_2) propagation stages (see § 3). These propagation rates were in that case calculated as :

a) $V_1 = L(T)/(T-T_{init})$, where T = time for tests interrupted during the slow propagation rate, or T = time of transition from slow to rapid stage when specimens were led to failure, T_{init} = initiation time, L(T) = crack depth at the time T.

b) $V_2 = (L(T)- L_{crit})/(T - T_{crit})$, where T = test time, L_{crit} = critical depth for transition from V1 to V2 (# 80 μm) and T_{crit} = time of transition from slow to rapid stage.

Creep tests were analysed from the classical curves of elongation versus time.

Hydrogen content of specimens was analysed quantitatively after some tests by classical melting techniques. The average accuracy of measurements was about 2 ppm.

3- DESCRIPTION OF CRACKING

In order to understand the mechanisms for SCC of Alloy 600, a detailed description of the cracking behaviour is needed, in both constant-load tests and CERTs. Some part of the following data, which concerns the tubes 6L and 6.242.R, has been described in detail elsewhere [23]. The main results obtained are summarized hereby.

Stages of cracking

Three stages are schematically observed during interrupted constant load tests and CERTs, on tubes with a superficial strain-hardened layer :

- First, a short initiation period is observed. This initiation period was arbitrarily defined, in correlation with the roughness of the tubes, as the time when no crack deeper than 10 μm occurred. It lasts about one hundred hours for constant load tests in pure water (figure 1) ; it lasts also about the same time for CERTs, in primary water with hydrogen overpressure, for strain rate from 5×10^{-9} to 10^{-6} s^{-1}. This initiation time was independent of strain rate and was slightly higher than the time required for the stabilisation of the rest potential observed in primary water without hydrogen (figure 2).

- Then follows a period of slow propagation rate, until the depth of the longer cracks reaches 50 to 80 μm. The duration of this stage, from a few hundreds to thousands of hours, depends on the stress level for constant-load tests (figure 1) and on the strain rate for CERTs.

- The last period is one of rapid propagation rate, generally leading to the rupture of the specimens. On tubes in the as-received surface condition, transition from the slow to the rapid propagation rate occurred at a crack depth of about 80 μm (figure 3).

Relationship between strain rate and crack propagation rate

The relationship between strain rate and crack propagation rate is given in table III. The rapid propagation rate is generally found to be about ten times higher than the slow one, and both show a dependency on the strain rate with a power law of 0.58 (figure 4). These results are in good agreement with previous results from Santarini [22], and from Combrade [24] who found a power law of 0.66 as predicted by electrochemical measurements, on the basis of a classical slip-step dissolution model. This was found to be a good support to the relevance of this model for cracking of Alloy 600.

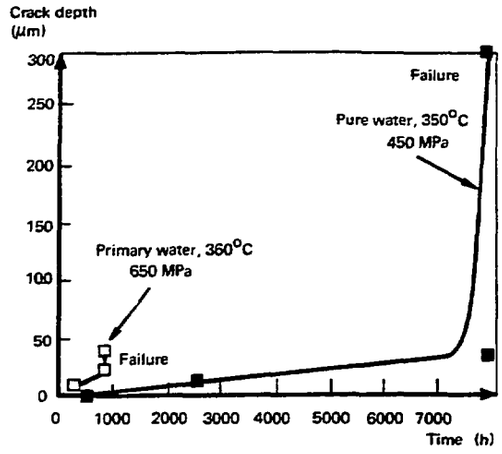

Figure 1 – Crack depth as a function of the duration of the constant-load test (tube 6L in the as-received surface state, 4 bar-overpressure of hydrogen at 125°C).

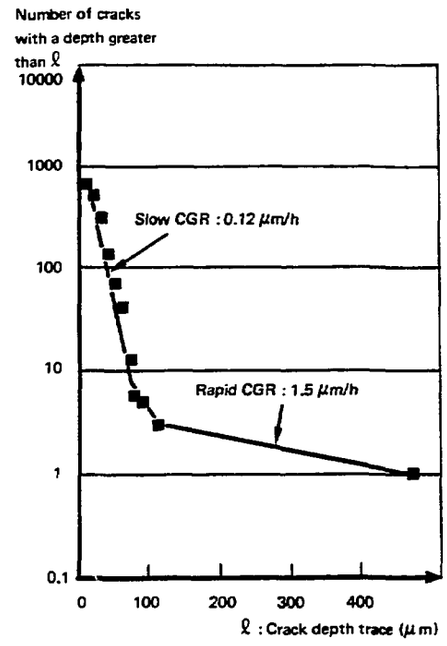

Figure 3 – Number of cracks with a trace depth greater than ℓ, as a function of ℓ (tube 6.242R in the as-received condition, CERT at 5.10^{-8} s^{-1}, primary water 360°C, 4 bar overpressure of hydrogen at 125°C).

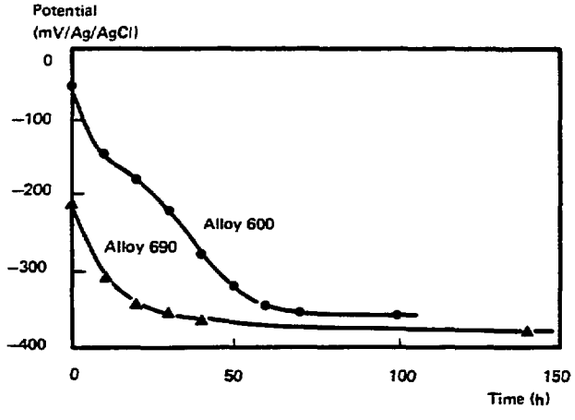

Figure 2 – Evolution of corrosion potential as a function of time (primary water without hydrogen, 350°C).

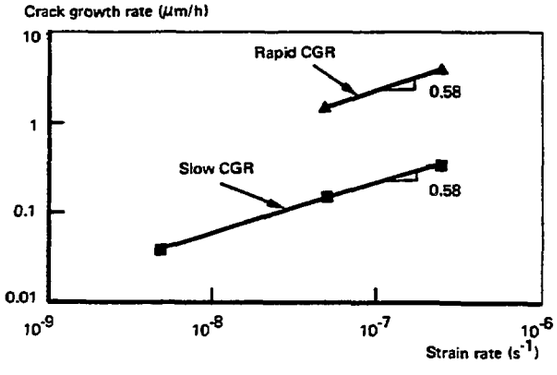

Figure 4 – Evolution of cracks growth rate as a function strain rate (tube 6.242R in the as-received condition, primary water 360°C, 4 bar overpressure of hydrogen at 125°C).

Table III : Relationship between strain rate and crack propagation rate during CERTs in 360°C primary water (+ 4 bar H_2 at 125°C) (tube 6.242.R)

Strain rate (s^{-1})	2.5×10^{-7}	5×10^{-8}
Low crack propagation rate (μm/h) : V_1	0.34	0.12
High crack propagation rate (μm/h) : V_2	3.87	1.50

4- EFFECT OF MECHANICAL PARAMETERS

Respective roles of stress and strain rate

It is very important for mechanism understanding to know which parameter, stress or strain rate, is the predominant one for crack growth rate. Slip-step dissolution mechanisms predict that the strain rate should control cracking. However, stress and strain rate are generally interdependent. To assess their intrinsic effects, specific experiments were performed, based on the comparison of the maximal crack depths obtained during tests carried out in the same range of stress level, but with different strain rates (CERTs), or with a strain rate corresponding to the creep obtained during constant-load tests. The detailed experiments, which involved complex loading procedures, are described elsewhere [23]. The results are summarized in figure 5. They demonstrate that the cracking, at least in the low-rate propagation phase, is much more dependent on the strain rate than on the stress. This is true of course, as long as the stress is above the threshold level.

Since the strain rate appears pr[illegible]erant, it was interesting to check if the susceptibility of the different heats of tubing was correlated to their creep behaviour. This was studied at 360°C on mill-annealed condition and on thermally-treated (16 h at 700°C) condition. Results are plotted in figure 6. A correlation seems to be obtained in the as-received condition : the higher creep rates are obtained on tubes 6L and 6.242.R which are the most susceptible to SCC, and a very low creep rate is obtained on tube 6E which is not susceptible. However, this correlation is not observed when the comparison is performed, on the same tube, between the mill-annealed and the thermally treated conditions. Localisation effects of strain to the grain boundary [25] and a possible interaction between creep and liquid environment should perhaps be taken into account.

Interaction between creep and liquid environment

A local interaction between plasticity and corrosion was demonstrated in some fatigue experiments but also in creep experiments on various alloys [26, 27]. Recent theories account for this type of interaction for SCC of stainless steels [17].

To check if the observation is relevant for Alloy 600, its creep behaviour was compared at 360°C in air and in primary water with a 4 bar-hydrogen overpressure. Tests were carried out on the tube 6L in the electropolished condition, for a stress level from 650 to 680 MPa. Results for the first 300 h are plotted in figure 7. Since the average scatter of creep in air is less than 50% after 200 h, these results seem to indicate a significant increase of creep in primary water compared to air. However, some slight cracks (maximum 10 μm after 1,000 h of test) were observed, and although their influence was probably negligible, the conclusion was not definitive. To make sure such an observation, the same comparison was performed on a tube of Alloy 690 at a stress level of 600 MPa. It did not crack at all after 4,000 h of test. Results (figure 8) show an increase of creep rate higher than a factor two in the presence of primary water.

So, an increase of creep rate of Alloy 600 in the presence of water seems to occur.

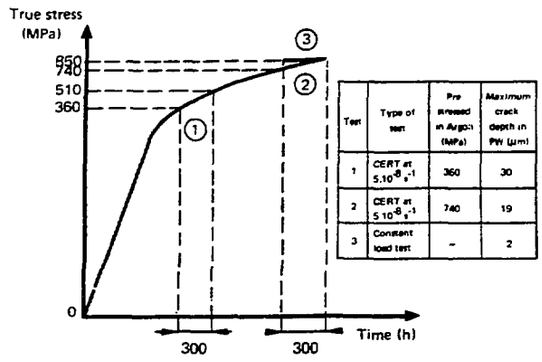

Test	Type of test	Pre stressed in Argon (MPa)	Maximum crack depth in PW (μm)
1	CERT at 5.10^{-8} s^{-1}	360	30
2	CERT at 5.10^{-8} s^{-1}	740	19
3	Constant load test	–	2

Figure 5 – Comparative crack depths during the slow propagation stage in CERT (5.10^{-8} s^{-1}) and constant-load tests (tube 6L in the electropolished conditions, primary water 360°C, 4 bar overpressure of hydrogen at 125°C).

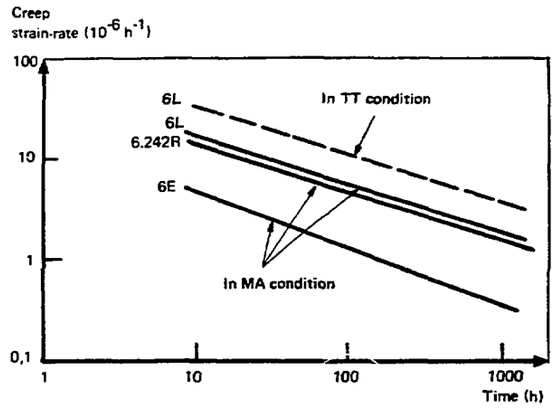

Figure 6 – Creep strain rate vs time, for three Alloy 600 tubes in the mill-annealed condition (360°C, nominal stress: 650 MPa).

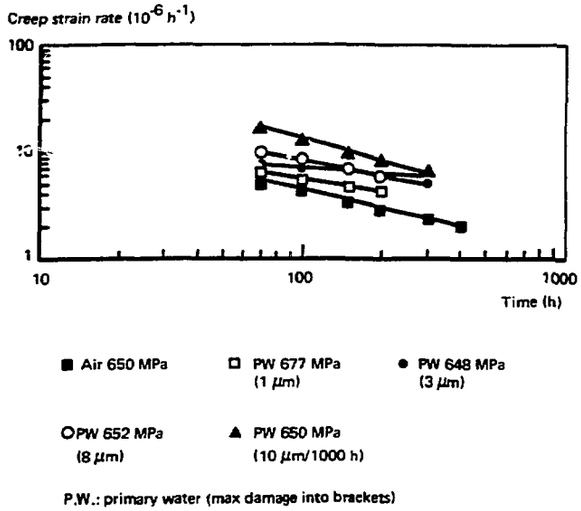

Figure 7 – Creep strain rate vs time for tube 6L in the electropolished condition (360°C, nominal stress: 650-680 MPa)

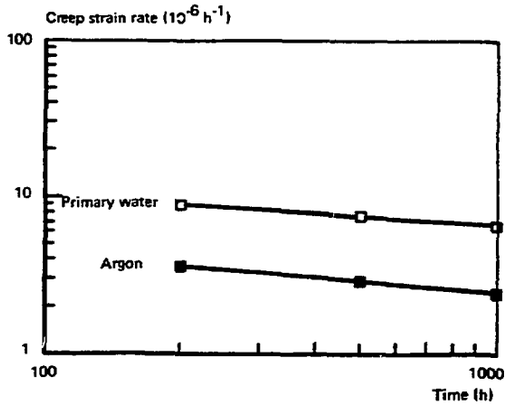

Figure 8 – Creep strain rate vs time for Alloy 690 in the electropolished condition (360°C, nominal stress: 600 MPa)

5 - EFFECT OF PHYSICO-CHEMICAL PARAMETERS

Effect of hydrogen

The effect of hydrogen was studied by carrying out CERTs and RUB tests, with a hydrogen overpressure ranging from 0 (in fact 0.005 bar as calculated from a 0.01 μm-loss of corroded metal during the test) to 20 bar. The corresponding dissolved hydrogen content calculated at test temperature was respectively 0.1 to 757 ppm. Results are reported table IV. For both tests, a maximum detrimental effect of hydrogen is found at intermediate overpressures and a decrease of SCC occurred at 20 bar overpressure.

Table IV : Effect of hydrogen overpressure on SCC behaviour of mill-annealed Alloy 600 (6.242.R) in primary water (1,000 ppm B, 2 ppm Li) at 360°C

a/ CERTs (2.5×10^{-7} s^{-1})

Hydrogen overpressure at 125°C (bar)	Calculated hydrogen in solution at 360°C (ml H_2 TPN/kg H_2O)	Calculated hydrogen in solution at 360°C (ppm)	Duration (h)	Ultimate tensile stress (MPa)	Elongation (%)	Secondary cracks depth (μm)	Main crack depth (μm)	Average crack velocity (μm/h)	Calculated crack velocity (μm/h)
without	1	0.1	369	723	30.8	46	50	0.14*	0.14**
1	420	38	352	638	28.9	89	95	0.27*	0.25**
4	1,660	151	321	690	30.3	140	235	- -	0.34** 3.9***
20	8,320	757	367	741	31.7	37	40	0.11*	0.10**

* velocity of the longest secondary crack
** velocity calculated according to Santarini [22]
*** velocity in the rapid stage

b/ RUB tests

Hydrogen overpressure at 125°C (bar)	Calculated hydrogen in solution at 360°C ml H_2 TPN/kg H_2O	 ppm	Initiation time * (h)	Time to failure (h)
without	1	0.1	> 4,250	no cracking in 4,250 h
1	420	38	< 500	< 500
4	1,660	151	500 < t < 1,000	500 < rupture < 1,000
20	8,320	757	< 1,000	< 1,000

* time required to get visible cracks

CERTs : Crack growth rates obtained from CERTs are reported Table IVa, and the distribution of crack lengths is plotted in figure 9. The slow-phase crack growth rate increases from 0 to 4 bar H_2-overpressure, then decreases by a factor 3.5 from 4 to 20 bar H_2. For a 20 bar-overpressure, the crack growth rate is lower than without hydrogen and as a consequence, hydrogen may seem to be not detrimental. However, the number of cracks is more than 3 times higher at 20 bar than at 0 bar-overpressure (figure 9). With a 4 bar-overpressure, a very long main crack was observed : a rapid propagation phase occurred, as usually (cf. § 3), when the crack length reached 80 μm. The rapid crack growth rate was calculated, using the distribution of cracks lengths (cf. § 2), and was found to be about ten times higher than the slow one.

RUBs : Results on RUBs (table IVb) confirm : the increase of susceptibility to SCC from 0 to 1 bar H_2 overpressure. and its decrease from 4 to 20 bar. However, the maximum susceptibility occurs at 1 bar, and not at 4 ; moreover, a great difference of susceptibility appears between 0 (no cracking) and 20 bar, contrary to results of CERTs. This difference could be due to the fact that initiation times are much longer for RUBs than for CERTs, and to a different effect of hydrogen on the initiation and propagation phases. Then these results could indicate a much more important effect of hydrogen on the initiation time than on the propagation rate.

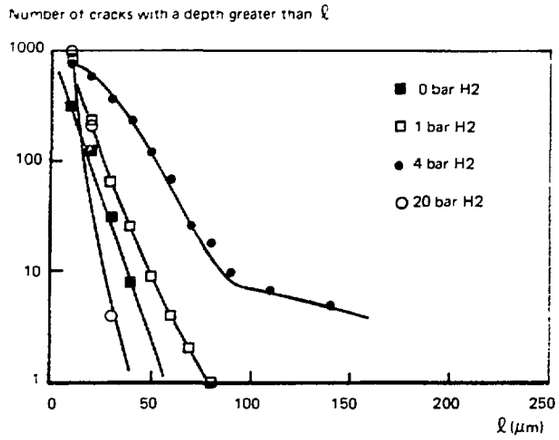

Figure 9 – Crack depth distributions ; CERT (2.5×10^{-7} s^{-1}); primary water 360°C with various hydrogen overpressures

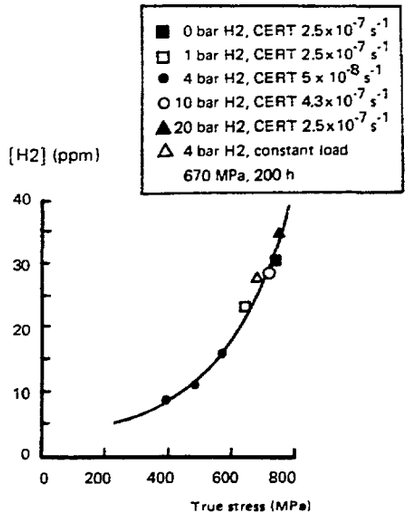

Figure 10 – Bulk hydrogen content as a function of the stress.

Figure 11 – Cleavage micro-facets on the grain boundary; CERT (2.5×10^{-7} s^{-1}); primary water 360°C + 1 bar H2 (A % = 29 %).

Figure 12 – Cleavage micro-facets on the grain boundary; CERT (5×10^{-8} s^{-1}); primary water 360°C + 4 bar H2 (A % = 15 %).

As a conclusion the results are in agreement with previous results [14, 28] showing an increase of susceptibility in pure water at low hydrogen overpressures. The decrease observed in this work at a 20 bar overpressure is quite new and was only observed, up to now, in 400°C steam.

Hydrogen absorption

The hydrogen uptake of specimens was measured after SCC tests by the classical melting method. Samples were taken in the central part on a length of about 50 mm. Results are reported in figure 10, as a function of the maximum stress reached during the test. The hydrogen content of specimens increases when the stress increases ; it is also in correlation with the maximum strain for CERTs. A striking point is that the hydrogen content does not depend on the hydrogen overpressure during the test : the highest levels are found for 0 and 20 bar overpressures and are almost the same, notwithstanding that they correspond to a minimum susceptibility to SCC. That raises questions about the meaning of the hydrogen measured in these experiments. At 360°C, the hydrogen solubility in Alloy 600, without stress, is about 2 to 4 ppm, which is far less than the values measured in these experiments. With high stresses at crack tip, the solubility should be locally increased, according to hydrogen cracking theories, but this effect disappears when failure occurs. So the hydrogen measured in these experiments corresponds probably to hydrogen trapped on dislocations or defects created by plastic deformation.

The absence of correlation between the hydrogen content of the specimens and the hydrogen overpressure or the test severity implies that the detrimental effect of hydrogen at intermediate overpressures is not directly related to an easier ingress of hydrogen in the material, which does not support the classical hydrogen theories. This point will be discussed later.

Influence of the sensitization to intergranular corrosion

The effect of sensitization was assessed, with and without hydrogen overpressure, by comparison of behaviour of the tube 6.242.R in the as-received condition (not sensitized) and in the thermally-treated condition (1 h 700°C, heavily sensitized). Results without hydrogen overpressure, obtained with CERTs, are reported Table Va. No detrimental effect of sensitization is observed, and the SCC behaviour of Alloy 600 is slightly improved. The beneficial effect of sensitization appears clearly from results obtained from RUBs at 1 to 20 bar hydrogen overpressures (Table Vb) : in all cases, the time to cracking increases compared to the as-received condition one.

This decrease of susceptibility with intergranular "dechromization" is difficult to explain by electrochemical factors in a slip-step dissolution model, but could be explained by the easier stress relief at grain boundaries when intergranular carbides concentration increases.

Oxygen effects

Some tests were carried out to assess the effect of a 4 bar-oxygen overpressure, with specimens in the mill-annealed and in the thermally-treated conditions (1 h 700°C). On RUBs, no cracks were obtained in any conditions after 3,000 h. A CERT carried out with a thermally treated tube (1 h 700°C) did not produce cracks (Table VI). Although these results are not sufficient to quantify precisely the effect of oxygen, they clearly indicate that the oxygen detrimental effect, if any, is not important compared to that of hydrogen.

This absence of detrimental effect of oxygen, especially in the sensitized condition, could seem to be in contradiction with previous results for Alloy 600 [29] or with the well-known detrimental effect of oxygen for sensitized stainless steels in BWR water. However, detrimental effects of oxygen from [29] were observed only in association with a crevice chemistry. Furthermore it was demonstrated [30] that sensitized Alloy 600 was susceptible to SCC at potentials corresponding to oxygenated solutions, only when an intergranular attack was performed before the test. It was also demonstrated [31] that SCC of sensitized stainless steels in pure water is strongly inhibited when temperature is higher than 300°C, except if water contains impurities. To check that point, a CERT was conducted in primary water with 20 ppm of chlorides and a 4 bar-oxygen overpressure on a mill-annealed specimen (table VI). Cracking occurred very quickly in that case. It proves that the oxygen detrimental effect occurs only when impurities are present.

Table V : Effect of sensitization on Alloy 600 (6.242.R) SCC behaviour in primary water (1,000 ppm B, 2 ppm Li) at 360°C

a/ CERTs (2.5×10^{-7} s^{-1}) ; no hydrogen overpressure

Heat treatment	Duration (h)	Ultimate tensile stress (MPa)	Elongation (%)	Secondary cracks depth (μm)	Main crack depth (μm)	Average crack velocity (μm/h)	Calculated crack velocity (μm/h)
mill-annealed	369	723	30.8	46	50	0.14*	0.14**
heat treated 1 h 700°C	423	678	36.6	32	40	0.09*	0.09**

* velocity of the longest secondary crack
** velocity calculated according to Santarini [22]

b/ RUB tests

Initial annealing	hydrogen overpressure at 125°C (bar)	Calculated hydrogen in solution at 360°C ml H_2 TPN/kg H_2O	ppm	Initiation time* (h)	Time to failure (h)
mill-annealed	1	420	38	< 500	< 500
heat treated 1 h 700°C				< 500	500 < rupture < 1,000
mill-annealed	4	1,660	151	500 < t < 1,000	500 < rupture < 1,000
heat treated 1 h 700°C				> 1,000	> 1,000
mill-annealed	20	8,320	757	< 1,000	> 1,000
heat treated 1 h 700°C				> 1,000	> 1,000

* see footnote table IVb.

Table VI : Effect of oxygen overpressure on SCC behaviour of Alloy 600 (6.242.R) in primary water (1,000 ppm B, 2 ppm Li) at 360°C ; CERTs (2.5×10^{-7} s^{-1})

Heat treatment	Environment	Calculated oxygen solubility ml O_2 TPN/kg H_2O	Duration (h)	Ultimate tensile stress (MPa)	Elongation (%)	Secondary crack depth (μm)	Main crack depth (μm)	Average crack velocity (μm/h)
heat treated 1 h 700°C	4 bar O_2 (a)	1,591	336	621	30.6	-	-	-
mill-annealed	4 bar O_2 + 20 ppm Cl^-	(2,274 ppm)	41	381	2.8	630	640	15.6*

(a) $[Cl^-]$: 0.7 ppm
*velocity of the main crack

6 - FRACTOGRAPHIC ASPECTS

Recent observations on fractographic aspects of transgranular cracking for various alloys showed evidence of discontinuous propagation. Several models implying a film-induced clivage or an interaction between corrosion and plasticity proposed an explanation for this discontinuous propagation and for the observed cristallographic aspects.
However, the cracking of Alloy 600 in primary water is intergranular. More recently, Magnin proposed an extension of his model, initially developed for transgranular cracking, to the intergranular cracking of fcc alloys [20]. This model predicts a periodic brittle microcracking which can be either intergranular or "pseudo-intergranular" on {111} plans, very near from the grain boundaries.

To check if such a facies was possible, examinations were performed using scanning electron microscope (SEM) on fracture surfaces ; the detailed results will be presented elsewhere [32]. The used samples were cracked using CERTs, in a primary water with a hydrogen overpressure from 0 to 20 bar. Most of the surfaces were merely intergranular, but approximately 10% of grain boundaries clearly presented microclivage facets. Some examples are shown in figures 11 and 12. Such facies are quite new for intergranular cracking of Alloy 600, and cannot be easily explained by a classical dissolution model.

7 - DISCUSSION

The compatibility of the results presented in this work with the various mechanisms is examined.

Slip-step dissolution

The main observed effect which could account for a slip-step dissolution mechanism is the preponderant effect of the strain rate on the crack growth rate (cf § 3), and the fact that the crack growth rate depends on the strain rate with a power law of about 0.6. This dependency was fairly well predicted from data with electrochemical measurements obtained by Combrade. However, this is not sufficient, because such a dependency could also result from a hydrogen mechanism : that would be the case if the corrosion rate controlled the ingress of hydrogen, or if the limiting parameter was the transport of hydrogen by dislocations. Such a dependency is also expected in mechanisms involving an interaction between corrosion and plasticity.

Another argument concerns the effect of chromium : this element improves the IGSCC resistance of nickel-base alloys [5] and is reputed to lower dissolution rate and to increase the passivation rate. However, it should be noticed that sensitization seems to be not detrimental, even when oxygen is present, despite chromium depletion at the grain boundaries. This behaviour could be explained by a positive structural effect (presence of intergranular carbides).

The relevance of slip-step dissolution mechanism does not seem to be invoked, as long as solubilities of iron (3 - 20 ppb), nickel (< 2 ppb) and chromium (0.2 ppb) are quite low in high temperature water. Moreover the detrimental effect of hydrogen between 0 to 4 bar has to be accounted for, since the increase of hydrogen pressure decreases the equilibrium potential and then the dissolution rate. One hypothesis which could solve this difficulty is that the dissolution rate- and then the crack growth rate - should be controlled by mass transport effects, depending on solubility limits of elements. Taking into account the iron solubility, the far more soluble element, the hydrogen effect could be explained from 0 to 4 bar by the Schickorr reaction :
$1/3\ Fe_3O_4 + (2 - b)\ H^+ + 1/3\ H_2 = Fe(OH)_b^{(2-b)+} + (4/3 - b)\ H_2O$, with $b = 0, 1, 2, 3, 4$.
The solubility of iron depends on $(pH_2)^{1/3}$, and the same dependency should be observed for crack growth rate. This relationship is not observed since the crack growth rate decreases from 4 to 20 bar. Smialowska [3] explained this decrease by the fact that a high overpressure of hydrogen could prevent nickel oxidation, and then Alloy 600 dissolution. This explanation is questionable if the origin of hydrogen comes from dissolution. If it does not come from corrosion, it is difficult to understand why the hydrogen content is independent from hydrogen overpressure.

Hydrogen-induced cracking

In this mechanism, the detrimental effect of hydrogen is directly correlated with its local concentration in the metal. The obtained results showing the detrimental effect of the hydrogen overpressure from 0 to 4 bar could accredit such a mechanism, on the condition that the hydrogen ingress in the sample increases with the overpressure. In fact the results of hydrogen analyses in the samples clearly contradict this interpretation since the most severe crackings are not correlated with the highest hydrogen ingress.

Moreover, the decrease of SCC susceptibility from 4 to 20 bar-overpressure cannot be easily explained by such a mechanism. A classical explanation is that a hydrogen overpressure above a certain level could decrease the corrosion rate, then the hydrogen ingress. This can also be refuted by the hydrogen analysis results, since the hydrogen content from specimens does not

depend directly on the hydrogen overpressure.
The conclusion is that a hydrogen-induced cracking mechanism does not correctly explain the behaviour observed in this work. But hydrogen seems to be important in reducing the initiation time, probably through a change in the passivation properties of the surface film.

Models implying plasticity

Since none of the classical models implying dissolution or hydrogen seems able to clearly explain the SCC of Alloy 600, attention has to be paid to other theories. The film-induced clivage model needs a dealloyed or porous film which is not proved on Alloy 600. The corrosion-plasticity-interactions models (Jones [16], Magnin [17, 20], Flanagan-Lichter [18] or Lynch [19]) allow to account for many counter-arguments of the dissolution model. They do not need an important dissolution of metal and may explain the non-detrimental effect of sensitization by stress relief. Such models, particularly those of Lynch and Magnin, could account for the strong influence of hydrogen on the initiation process by adsorption. And above all, the observed environmental-assisted creep is consistent with these models.

The main argument against these models is the fractographical aspect of the crack facies, all of them predicting a transgranular cracking. The Magnin's model [20] was improved to account for pseudo-intergranular cracking of Alloy 600, with clivage-like facets. Nevertheless, if such a model is involved, many questions still arise : (i) why SCC of Alloy 600 in water never appears transgranular ? (ii) the clivage-like facets were only observed on nearly 10% of the facies, (iii) the cristallographic plans of the clivage-like facets must be determined to check if they are those predicted by the model {111}.

The consequences of this model have to be better assessed, particularly to account for the complexity of the hydrogen influence on propagation.

8 - CONCLUSION

The object of this study was first to get a precise knowledge of the different stages of cracking and their dependence on various parameters, and then to analyze the compatibility of the results with the main mechanisms which had to be considered.

Results showed three stages in cracking : an incubation time, a slow-rate propagation period followed by a rapid-rate propagation stage. Tests separating stress and strain rate contributions demonstrated that the strain rate is the main parameter which controls the crack propagation.

The hydrogen overpressure effect on the propagation was found to be maximum at 1 or 4 bar, but a strong decrease was observed at 20 bar. Analyses of the hydrogen ingress in the metal showed that it was neither correlated to the hydrogen overpressure nor to the severity of the cracking. This seems to demonstrate that a direct detrimental effect of hydrogen on cracking is not involved.

Finally, none of the classical mechanisms, neither hydrogen-assisted cracking nor slip-step dissolution, can correctly describe the observed behaviour. Some fractographic observations, and an observed influence of primary water on the creep rate of Alloy 600 lead to think that other recent mechanisms, involving an interaction between dissolution and plasticity, have to be considered.

REFERENCES

[1] H. Coriou, L. Grall, Y. Legall, S. Vettier, 3rd Colloque of Metallurgy, Saclay 1959, North Holland Publishing, Amsterdam (1960), p. 161.

[2] R. Bandy, D. Van Rooyen, J. Materials for Energy Systems 7 (3), 237 (1985).

[3] Z. Szklarska-Smialowska, 4th Int. Symposium on Environmental Degradation of Materials in Nuclear Power Systems-Water Reactors, Jekyll Island, GA, 6-10 August 1989, Ch. 6, pp. 1-24.

[4] R.W. Staehle, in Materials Performance Maintenance, Pergamon Press, New York, 1991, pp. 3-43.

[5] J.M. Gras, in Parkins Symposium on Fundamental Aspects of Stress Corrosion Cracking, ed. S.M. Bruemmer et al., TMS, 1992, pp. 411-432.

[6] Y.S. Garud, T.L. Gerber, EPRI final Report NP-3057, May 1983 ; Corrosion 42, 99 (1986) ; Corrosion 46, 968 (1990).

[7] J.A. Begley, EPRI final Report NP-7008, October 1990.

[8] F.P. Ford, EPRI Report NP-2589, September 1982.

[9] P. Combrade, O. Cayla, M. Foucault, A. Gelpi, G. Slama, 3rd Int. Symposium on Environmental Degradation of Materials in Nuclear Power Systems-Water Reactors, Traverse City, 30 August-3 September 1987, pp. 525-533.

[10] P. Combrade et al, 4th Int. Symposium on Environmental Degradation of Materials in Nuclear Power Systems-Water Reactors, Jekyll Island, GA, 6-10 August 1989, Ch. 5, pp. 79-95.

[11] P.L. Andresen, Corrosion/Nace 89, Paper 566, New-Orleans, 17-21 April 1989.

[12] W.K. Lai, Z. Szklarska-Smialowska, Corrosion 47, 40 (1991).

[13] P. Berge, Proc. of Nace Symposium on Life Prediction of Corrodible Structures, Cambridge, 23-26 September 1991.

[14] N. Totsuka, Z. Szklarska-Smialowska, Corrosion 43 (1987), 734-738.

[15] C.H. Shen, P.G. Shewmon, Metallurgical Transactions A 21A, 1261, (1990) ; 22A, 1857, (1991).

[16] D.A. Jones, Metallurgical Transactions A 16A, 1133, (1985).

[17] T. Magnin, R. Chierragatti, R. Oltra, Acta Metall., 38, 1313, (1990).

[18] W.F. Flanagan, P. Bastias, B.D. Lichter, Acta Metall., 39, 695, (1991).

[19] S.P. Lynch, Acta Metall., 36, 2639, (1988).

[20] T. Magnin, "A unified model of the trans and intergranular stress corrosion cracking in FCC ductile alloys", this conference.

[21] G.S. Upadhyaya, R.K. Dube, "Problems in Metallurgical Thermodynamics and Kinetics", p. 48, Pergamon Press, New York, (1977).

[22] G. Santarini, Corrosion 45, 369 (1989).

[23] J-M. Boursier, J-M. Gras, F. Vaillant, Eurocorr'92, Espoo June 1-4 1992, Vol. II, p.11.

[24] P. Combrade, M. Foucault, et al., PWS 4-A3, Technical meeting, Pittsburgh, May 1987.

[25] D. Garriga-Majo, B Raval, J.C. Van-Duysen, D. Caldemaison, Comptes Rendus de l'Académie des Sciences, Paris, t. 311, Série II, p. 637, 1990.

[26] R.W. Revie, H.H. Uhlig, Acta Metall., 22, 619, (1974).

[27] T. Magnin, Matériaux et Techniques, 11-12, 41, (1989).

[28] G. Economy, R.J. Jacko, J.A. Begley, F.W. Pement, Corrosion 87, San Francisco, March 9-13, 1987.

[29] H.R. Copson, G. Economy, Corrosion, 24, 55 (1968).

[30] T. Shoji, S. Mori, Proc. of Nace Symposium on Life Prediction of Corrodible Structures, Cambridge, 23-26 September 1991.

[31] P.L. Andresen, Corrosion 92, paper n° 89, Nashville, April 26-May 1, 1992

[32] T. Magnin, D. Noel, R. Rios, "Microfractographic aspects of IGSCC of Alloy 600 in PWR Environment", to be published.